Bioconjugate Chemistry

Communication

pubs.acs.org/bc

Development of U11-Functionalized Gold Nanoparticles for Selective Targeting of Urokinase Plasminogen Activator Receptor-Positive Breast Cancer Cells

Svetlana Avvakumova,[†,∥] Elisabetta Galbiati,[†,∥] Laura Pandolfi,[†] Serena Mazzucchelli,[‡] Marco Cassani,[†] Alessandro Gori,[§] Renato Longhi,[§] and Davide Prosperi*[,†]

[†]NanoBioLab, Dipartimento di Biotecnologie e Bioscienze, Università di Milano-Bicocca, Piazza della Scienza 2, 20126 Milano, Italy

[‡]Dipartimento di Scienze Biomediche e Cliniche "Luigi Sacco", Università di Milano, Via G. B. Grassi 74, 20157 Milano, Italy

[§]CNR-ICRM, Via Mario Bianco, 9, 20131, Milan, Italy

Supporting Information

ABSTRACT: The functionalization of colloidal nanoparticles with short peptides often fails in achieving satisfactory targeting efficiency and selectivity toward receptor-specific human cells. Here, we show that an optimized passivation of gold nanoparticle surface with a mixed self-assembled monolayer, including a targeting ligand, a fluorescent dye, and an intercalating short PEG derivative, led to a very stable, nontoxic, and efficient nanoconjugate for targeting urokinase plasminogen activator receptor-positive breast cancer cells.

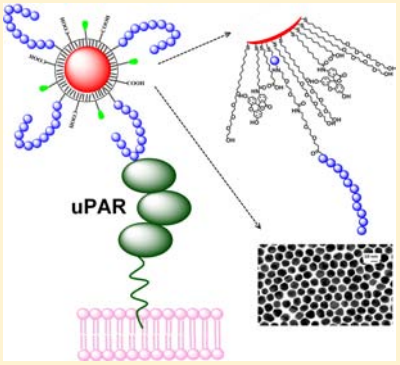

Cancer has become a major public health problem in many countries. Statistically, such cancers as pancreatic, liver, and lung lead to an extremely high level of morbidity and mortality (up to 97%), while breast cancer is most frequently diagnosed, being the leading cause of death for cancer among females.[1] Although targeted therapy with monoclonal antibodies is rapidly becoming the major nonsurgical treatment in many cancers,[2,3] the use of short peptides as targeting ligands of tumor receptors has several potential advantages over commonly employed entire antibodies. In particular, when more sophisticated nanoconjugates are used for drug delivery purposes, short peptides allow for regular and density-controlled distribution of ligands and lower immunogenicity of the nanoconstruct, along with their low nonspecific uptake by the reticuloendothelial system, such as the liver, spleen, and bone marrow. These features have led to their wide application as promising ligands for tumor targeting.[4] In addition, peptides are chemically stable and relatively easy to modify compared to monoclonal antibodies.[5]

A number of peptide-based ligands for cancer cell targeting have been described in the literature, with the most prominent examples being the arginine−glycine−aspartate (RGD) family of peptides for $\alpha_v\beta_{3/5}$ integrin receptor-targeting.[6−9] Peptide sequences derived from urokinase plasminogen activator (uPA) amino-terminal protein fragment (ATF) have recently been used as an efficient way of targeting the uPA receptor (uPAR) on cancerous cells.[10,11] uPAR was found overexpressed across a variety of tumor cells and tissues, including breast, lung, pancreas, liver, and stomach.[7] Moreover, such a high level of expression is considered to be associated with cancer invasion and metastasis.[12−16] Among uPAR-targeting peptide sequences, U11 peptide (VSNKYFSNIHW) represents a prominent part of the recognition fragment in uPA. Its loop-like structure comprises 11 amino acid residues localized at the tip of a β-hairpin loop within the growth factor domain of uPA. The interaction between U11 and uPAR was reported to be characterized by an equilibrium dissociation constant, K_d, of 1.3−1.4 μM.[10]

Thanou and co-workers used a U11 peptide−lipid amphiphile for functionalization of liposomes with the aim of nucleic acid delivery.[10] Although, the authors have obtained an efficient targeting of prostate cancer cells by the U11-functionalized nanoconjugates, still they indicated the presence of strong nonspecific interactions that caused an undesired binding of nanoparticles to the cell membranes. In addition, U11 peptide was shown to form β-sheets on the surface of liposomes when inserted at high densities. However, at low concentrations (1 mol %), the same peptide−lipid conjugates appear to rearrange into more separated structures inside the liposome bilayer.[10] Similarly, Mazzucchelli et al. have observed that direct random conjugation of U11 linear peptide to

Received: May 6, 2014
Revised: July 31, 2014
Published: July 31, 2014

dx.doi.org/10.1021/bc500202b | *Bioconjugate Chem.* 2014, 25, 1381−1386

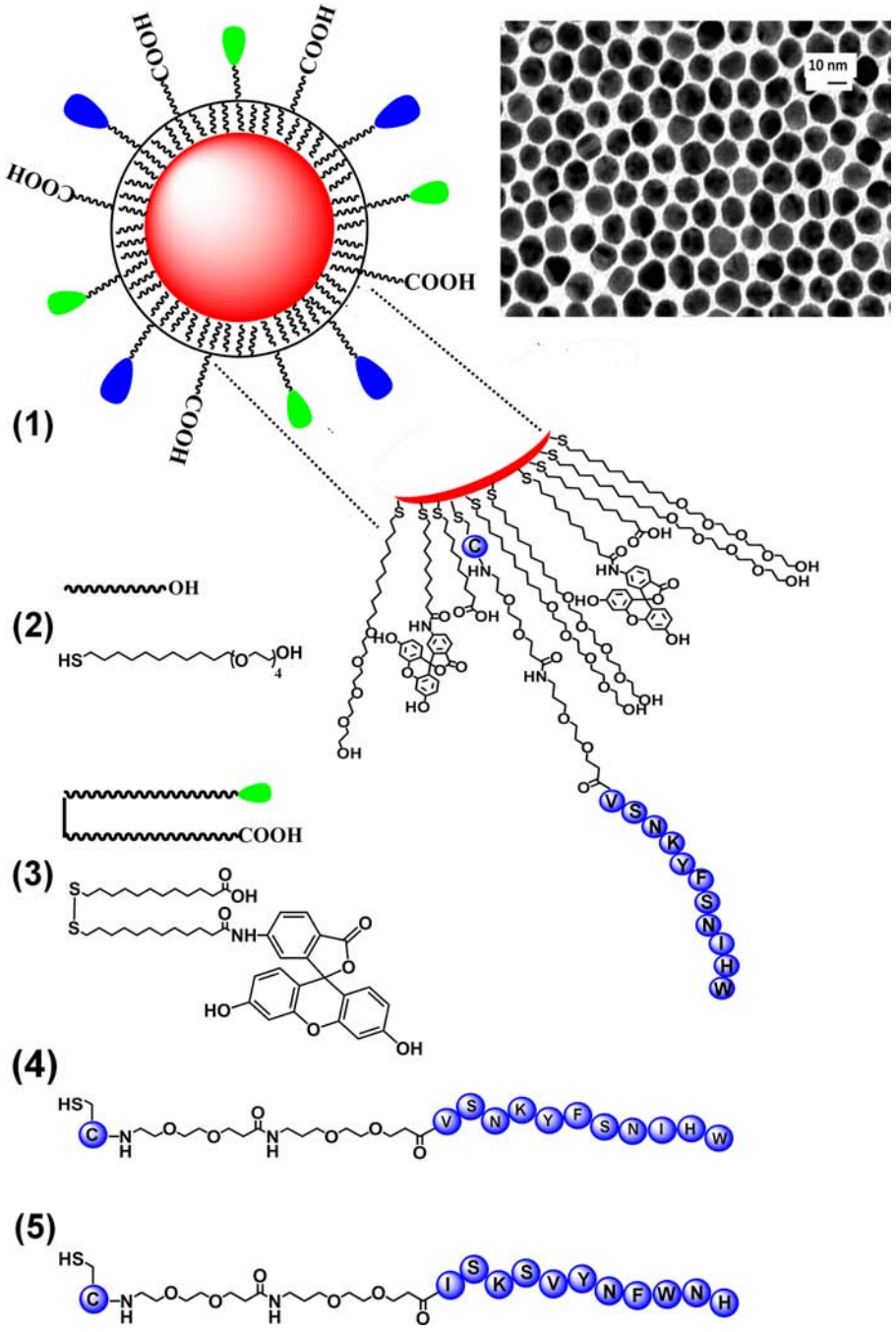

Figure 1. Schematic representation of fluorescent U11 peptide-functionalized Au-(**1**) NPs. A zoomed section of AuNP surface shows the supposed self-assembled organization of the mixed ligand monolayer. Chemical structures and amino acid sequences of the ligands and an example of TEM micrograph of AuNPs (inset) are included.

colloidal nanoparticles led to neither efficient nor selective binding of uPAR-positive cells in comparison with a uPAR-negative control, probably owing to a disadvantageous arrangement of the peptide or low availability for recognition.[17] In that case, likely the number of peptide molecules conjugated to the particle was too low to ensure successful targeting of the cells. Therefore, it is evident that the structure of the targeting molecule and its density and/or distribution on the nanoparticle surface play an important role both in colloidal stability and in the interaction with membrane receptors of the cell.[18,19]

Considering the high binding affinity of uPAR−uPA complex along with the favorable propensity of such complex to be endocytosed by receptor activation, the uPAR−U11 receptor−ligand system could be attractive for the design of smart nanoconjugates selective for uPAR targeting. Among different nanoparticles, gold nanoparticles (AuNPs) are a promising tool for biomedical applications, due to their unique optical and chemical properties, along with straightforward preparation and surface functionalization via Au−thiol chemistry.[20] In addition, the functionalization of nanoparticles with bioactive targeting ligands allows researchers to improve not only the selectivity of the conjugates exploiting a higher capacity to enter the cells but also their antitumor activity over the free drug through an increase of its local concentration.[21,22] However, no AuNPs-

dx.doi.org/10.1021/bc500202b | *Bioconjugate Chem.* 2014, 25, 1381−1386

based anticancer drug has been approved for clinical therapy yet except for only two AuNPs-containing drugs which have been in phase 0 (pilot study) and phase 1 of clinical trials. AuroShell nanoparticles have been investigated by Nanospectra Biosciences Inc. as potential tool for near-infrared photothermal therapy of head and neak cancers.[22] On the other hand, CytImmune Sciences Inc. has developed tumor necrosis factor (TNFα) bound AuNPs, namely, CYT-6091 Aurimmune, and Taxol and TNFα-bound colloidal gold, namely, and CYT-21001 (Auritol), for the treatment of solid tumors by breaking down tumor defenses.[22]

In this paper, we show that biocompatible fluorescent AuNPs can be successfully functionalized with U11 peptide with the aim of efficient targeting of uPAR-positive cancer cells. We developed an ad hoc nanoconjugate in which U11 peptide was inserted into a mixed monolayer of ligands imparting the required stability and fluorescent properties to AuNPs. Here, U11 peptide molecules were spaced by a short-chain PEG derivative containing both −SH and −OH groups, whose polarity favors the formation of a continuous passivation layer around nanoparticles. The high surface density of PEG chains provided AuNPs with an optimal colloidal stability, allowing them to reduce protein adsorption and nonspecific interactions with nontargeted biological species.[23−26] These features conferred also a more regular distribution of the peptide on the nanoparticle surface, which presumably avoided β-sheets formation resulting in a stronger affinity of immobilized U11 for uPAR. Finally, a fluorescein-modified bis-carboxylic disulfide was used to introduce a fluorescent moiety into the ligand shell, useful for further biological experiments (Figure 1).

U11 peptide was assembled by Fmoc-based solid phase peptide synthesis (see Supporting Information) adding an extra-sequence short PEG spacer in order to separate the main peptide chain from the nanoparticle surface, while an N-terminal cysteine residue was added to allow peptide covalent conjugation to AuNPs exploiting Au−thiol chemistry (Figure 1). A scrambled U11 variant (ISKSVYNFWNH) (**5**) was used as a negative control. Citrate-stabilized AuNPs were prepared by a modified Turkevich−Frens method, in which the reaction parameters were adjusted to yield monodisperse spherical nanoparticles of 16 ± 1.2 nm.[27−29] AuNPs were subsequently stabilized and functionalized by a mixed layer of ligands to give fluorescent Au−U11 nanoconjugates (**1**).[23,30] For this purpose, the components were mixed at specific stoichiometric ratios to achieve precise control over the number of functional ligands on each particle, maintaining reproducibility in the nanoparticle production. A short heterobifunctional PEG (11-mercaptoundecyltetra(ethylene glycol) (**2**)), containing both −SH and −OH groups, a fluorescein-bearing bis-carboxylic disulfide molecule (**3**), and Cys-modified U11 peptide (**4**) were used for nanoparticle derivatization. A typical schematic multifunctional nanoparticle, a TEM micrograph of the nanoparticles, and the chemical structure of the ligands utilized for the synthesis are schematically illustrated in Figure 1.

Although conjugation of peptides to the protecting ligand shell of AuNPs is an appealing strategy to preserve their biological activity, we have already had experience in successfully attaching biologically active thiol-containing peptides and proteins directly to the gold surface, observing retained biological functionality.[31,32]

It has been demonstrated that ligand shell composition and ligand density on nanoparticle surface play an important role in targeting efficiency and particle internalization mechanism.[33,34] Our preliminary experiments suggested to us that 3% of FITC groups is the most suitable amount to render the nanoparticles bright enough for binding studies in cells avoiding false positive results (Figure S8, Supporting Information). On the other hand, on the basis of these preliminary data, the U11 peptide amount for further experiments was established to be 3%. More details on the rationale of using this peptide density are reported in the discussion part of the paper. Furthermore, Au−U11 NPs containing 3% U11 peptide, 3% FITC, and 94% HS-PEG-OH ligands are named Au-(**1**) NPs.

In Table 1, representative characteristics of nanoparticles functionalized with different amounts of U11 peptide are summarized. Our results show that it is possible to obtain stable colloidal nanoparticles reaching a maximum 20% of peptide in the ligand shell. However, the insertion of U11 peptide at higher densities (>20%) resulted in poor stability of nanoparticles and their aggregation occurred shortly after functionalization.

Table 1. Characterization of Au−U11 Nanoparticles Containing Different Amounts of U11 Peptide by UV−Visible Spectroscopy, Transmission Electron Microscopy (TEM), Dynamic Light Scattering (DLS), and ζ-Potential

U11, %	SPR, nm	TEM, nm	DLS, nm	ζ-potential, mV
3	524	16 ± 1.2	21.3 ± 1.56	−30.36 ± 1.02
10	524	16 ± 1.2	21.1 ± 1.24	−23.74 ± 3.12
20	524	16 ± 1.2	23.1 ± 1.54	−18.96 ± 1.38

Although AuNPs are known to quench the dye fluorescence because of energy transfer effects,[35,36] we succeeded in obtaining sufficiently bright nanoparticles suitable for biological experiments. Only freshly prepared AuNPs were used for all biological experiments to avoid false negative results. The quenching efficiency of Au-(**1**) NPs was determined by plotting fluorescence spectra from nanoparticles before and after dissolution of the core. The very low intensity of emission peak from Au−U11 NPs grew considerably when the gold core was dissolved in aqua regia (Figure S5, Supporting Information), corresponding to a quenching efficiency of 98.4%.

The physicochemical properties of Au−U11 NPs have been studied by UV−vis, TEM, DLS, and ζ potential techniques. All the particles exhibited a negative charge and a small hydrodynamic diameter, indicating good colloidal stability and a highly monodisperse distribution under physiological conditions (150 mM NaCl at pH 7). To confirm the good colloidal stability of Au-(**1**) NPs, the particles were incubated with NaCl in a 150 mM to 1.5 M concentration range, and UV−vis spectra alterations were evaluated. In addition, nanoparticle stability in cell culture medium was studied by incubating Au-(**1**) NPs with high glucose DMEM lacking phenol red indicator and supplemented with 50% FBS. As shown in Figure S3 (Supporting Information), the particles are perfectly stable both in cell culture medium and even at the highest salt concentrations, since no UV−vis spectra alterations can be noticed.

To assess biological activity of Au-(**1**) NPs, we used uPAR positive human MDA MB 468 cells, uPAR positive murine 4T1 cells, and uPAR negative CAL51 breast cancer cells. In order to exclude possible cytotoxic effects of the particles, cell death was evaluated by annexin V assay after 1, 3, 24, 48, and 72 h of incubation (Figure 2a). No evidence of cytotoxicity was

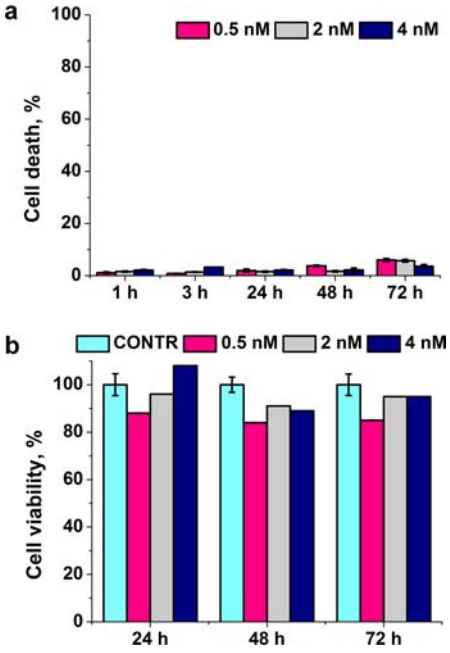

Figure 2. (a) Cell death assay with Au-(**1**) NPs. MDA MB 468 cells were treated with Au-(**1**) NPs (0.5, 2, and 4 nM) for 1, 3, 24, 48, and 72 h. Cell death was assessed to measure the exposure of annexin V evaluated by flow cytometry. The percentage of cell death in untreated population was subtracted. Data are expressed as mean values ± SD of three individual experiments. (b) Cell viability assessed by the MTT assay with Au-(**1**) NPs. MDA MB 468 cells were treated with Au-(**1**) NPs (0.5, 2, and 4 nM) for up to 72 h. The results are expressed as mean values ± SE of six individual experiments. Untreated cells are shown as negative control.

observed in MDA MB 468 cells after short incubation times at the dosages used (0.5, 2, and 4 nM). On the other hand, the nanoparticles induced minimally acceptable in vitro cytotoxicity after longer periods postincubation (24−72 h). As a control experiment, the same assay was performed also on uPAR-negative CAL51 cells, while control Au-PEG NPs were incubated with uPAR-positive MDA MB 468 cells (Figure S11 and Figure S12, respectively, Supporting Information). As indicated in Figure S12, Au−PEG NPs show similar cell death values as Au−U11 NPs after long incubation times, confirming the safety of as-prepared particles to the cells. A cytotoxicity study was performed with a conventional methylthiazolyl-diphenyltetrazolium bromide (MTT) based assay that relies on the color change of MTT by mitochondrial succinate dehydrogenase. The results show that Au-(**1**) NPs are not toxic at commonly used concentrations (Figure 2b).

In addition, in order to ensure that the presence of U11 peptide in the ligand shell does not affect the cytotoxicity of Au-(**1**) NPs, MTT assay with Au-PEG NPs, on MDA MB 468 cell line, as negative control was performed (Figure S13, Supporting Information). The results show a negligible difference between treated and untreated cellular viability profiles, indicating that Au−PEG NPs hardly affect cell profileration.

The binding efficiency between uPAR and Au-(**1**) NPs was studied by fluorescence-based flow cytometry (FACS) as a function of nanoparticle concentration. Cell-associated FITC fluorescence was examined 2 h after incubation of particles with the cells. Our aim was to assess the extent of receptor labeling minimizing nonmediated endocytosis. Hence, cell incubation with nanoparticles was performed at 4 °C. Flow cytometry results are summarized in Figure 3. First, we tested AuNPs containing higher densities of U11 in the ligand shell (5−20%)

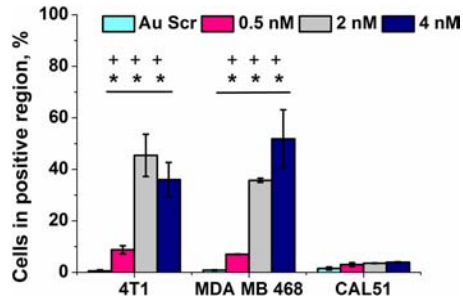

Figure 3. FACS analysis of uPAR targeting with Au-(**1**) NPs on MDA MB468 ($uPAR^+$), 4T1 ($uPAR^+$), and CAL-51 ($uPAR^-$) cells. The cells were incubated for 2 h at 4 °C with 0.5, 2, and 4 nM nanoparticle concentration. The results are expressed as mean values ± SD of three individual experiments normalized on cell proliferation of untreated cells. Student *t* analysis results are calculated and compared to $uPAR^-$ cells (*) and Au-Scr NPs (+).

with the aim to observe a possible binding improvement as a function of ligand density (Figure S8, Supporting Information). However, at very high peptide densities (10−20%) the nanoparticles showed a nonspecific binding to both uPAR-positive (MDA MB 468 and 4T1) and uPAR-negative (CAL51) cells. Importantly, when the U11 amount reaches 20%, the cells show strong aggregation, making it difficult to perform the analysis. This can be explained by a disadvantageous distribution of U11 amino acid sequences on the nanoparticle surface, as it has been already observed by Thanou et al.[6] On the other hand, at lower peptide densities (1%), the binding efficiency was not sufficiently high, probably because of insufficient nanoparticle avidity toward uPAR (Figure S8, Supporting Information). In contrast, treatment of $uPAR^+$ cells with AuNPs containing 3% of U11 peptide produced the most reliable data showing a 2-fold increase in the percentage of cells in the positive region compared to uPAR-negative treated cells (CAL51) at 0.5 nM concentration of AuNPs. At 2 and 4 nM nanoparticle concentration, the percentage of cells in the positive region grew to 53%, indicating the binding in a concentration-dependent manner (Figure 3). Importantly, nanoparticles functionalized with 3% scrambled U11 peptide (**5**) showed negligible binding to all kinds of tested cells, confirming the specificity of Au-(**1**) NPs for uPAR.

While flow cytometry is a powerful tool to quantify association of nanoparticles with cells, it does not distinguish between cellular binding and cellular internalization. To confirm cellular uptake and internalization of nanoparticles by breast cancer cells, we performed confocal laser scanning microscopy experiments. Scrambled peptide-conjugated nanoparticles (Au-**scr**) and cell-only controls were also included. The data do indicate the active involvement of a receptor-mediated targeting and U11 specificity to uPAR-positive MDA MB 468 cells, as Au-(**1**) NPs can be observed inside the cell. Negligible internalization was evident with nontargeted Au-**scr** NPs (Figure 4). More images are available in Figure S9, Supporting Information.

In summary, we have presented a robust method for the preparation of urokinase plasminogen activator receptor (uPAR) directed gold nanoparticles for targeting of breast cancer cells. The nanoparticles were functionalized with a short 11-amino acid (U11) peptide derived from the growth factor

dx.doi.org/10.1021/bc500202b | *Bioconjugate Chem.* 2014, 25, 1381−1386

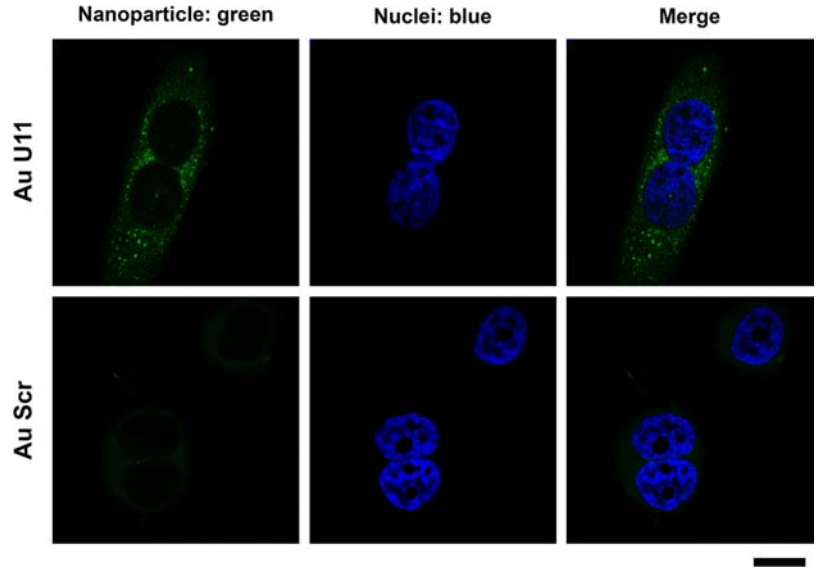

Figure 4. Confocal microscopy study of uPAR targeting with Au-(**1**) and Au-**scr** nanoparticles on MDA MB468 (uPAR$^+$) cells. The cells were incubated for 1 h at 37 °C with 2 nM nanoparticle concentration. Nuclei were stained with 4′,6-diamidino-2-phenylindole (DAPI). Scale bar = 10 μm.

domain of uPA, which is responsible for binding to uPAR due to its epitopal folding. We show that an optimized insertion on gold nanoparticle surface of a 3% U11 in a mixed self-assembled ligand monolayer, including fluorescent dye and intercalating short PEG chains, led to very stable and nontoxic nanoconjugates, which promoted receptor selectivity for improved cell binding and uptake in uPAR-positive cancer cells. The next step will be to prove the efficiency of the optimized U11 nanoparticles for in vivo administration to uPAR-overexpressing breast cancer.

■ ASSOCIATED CONTENT

Supporting Information

Experimental details, HPLC analysis, UV−vis and fluorescence spectra, colloidal stability data, quenching efficiency data, cellular uptake quantification by ICP-AES, confocal microscopy images, and cell death and cell proliferation data. This material is available free of charge via the Internet at http://pubs.acs.org.

■ AUTHOR INFORMATION

Corresponding Author

*E-mail: davide.prosperi@unimib.it.

Author Contributions

‖S.A. and E.G. contributed equally.

Notes

The authors declare no competing financial interest.

■ ACKNOWLEDGMENTS

This work was supported by Fondazione Regionale per la Ricerca Biomedica (FRRB), the “NanoBioSense” Project (Sardegna-Lombardia), and Cariplo Foundation (“The MULAN Program”, Project No. 2011-2096). S.A. acknowledges a research fellowship from Nerviano Medical Sciences S.r.l. We thank R. Allevi (CMENA, University of Milan, Italy) for TEM.

■ REFERENCES

(1) Jemal, A., Bray, F., Center, M. M., Ferlay, J., Ward, E., and Forman, D. (2011) Global cancer statistics. *Ca—Cancer J. Clin. 61*, 69−90.

(2) Scott, A. M., Wolchok, J. D., and Old, L. J. (2012) Antibody therapy of cancer. *Nat. Rev. Cancer 12*, 278−287.

(3) Vanneman, M., and Dranoff, G. (2012) Combining immunotherapy and targeted therapies in cancer treatment. *Nat. Rev. Cancer 12*, 237−251.

(4) Stefanidakis, M., and Koivunen, E. (2004) Peptide-mediated delivery of therapeutic and imaging agents into mammalian cells. *Curr. Pharm. Des. 10*, 3033−3044.

(5) Aina, O. H., Sroka, T. C., Chen, M.-L., and Lam, K. S. (2002) Therapeutic cancer targeting peptide. *Biopolymers 66*, 184−199.

(6) Desgrosellier, J. S., and Cheresh, D. A. (2010) Integrins in cancer: biological implications and therapeutic opportunities. *Nat. Rev. Cancer 10*, 9−22.

(7) Danhier, F., Le Breton, A., and Préat, V. (2012) RGD-based strategies to target alpha(v) beta(3) integrin in cancer therapy and diagnosis. *Mol. Pharmaceutics 9*, 2961−2973.

(8) Lee, M. H., Kim, J., Han, H. J., Bhuniya, S., Sessler, J. L., Kang, C., and Seung Kim, J. (2012) Direct fluorescence monitoring of the delivery and cellular uptake of a cancer-targeted RGD peptide-appended naphthalimide theragnostic prodrug. *J. Am. Chem. Soc. 30* (134), 12668−12674.

(9) Park, J., Singha, K., Son, S., Kim, J., Namgung, R., Yun, C.-O., and Kim, W. J. (2012) A review of RGD-functionalized nonviral gene delivery vectors for cancer therapy. *Cancer Gene Ther. 19*, 741−748.

(10) Wang, M., Lowik, D. W. P. M., Miller, A. D., and Thanou, M. (2009) Targeting the urokinase plasminogen activator receptor with synthetic self-assembly nanoparticles. *Bioconjugate Chem. 20*, 32−42.

(11) Wang, M., Miller, A. D., and Thanou, M. (2013) Effect of surface charge and ligand organization on the specific cell-uptake of uPAR-targeted nanoparticles. *J. Drug Targeting 21*, 684−692.

(12) LeBeau, A. M., Duriseti, S., Murphy, S. T., Pepin, F., Hann, B., Gray, J. W., VanBrocklin, H. F., and Craik, C. S. (2013) Targeting uPAR with antagonistic recombinant human antibodies in aggressive breast cancer. *Cancer Res. 73*, 2070−2081.

(13) Rao, J. S., Gondi, C., Chetty, C., Chittivelu, S., Joseph, P. A., and Lakka, S. S. (2005) Inhibition of invasion, angiogenesis, tumor growth, and metastasis by adenovirus-mediated transfer of antisense uPAR and MMP-9 in non-small cell lung cancer cells. *Mol. Cancer Ther. 4*, 1399−1408.

(14) Cantero, D., Friess, H., Deflorin, J., Zimmermann, A., Bründler, M. A., Riesle, E., Korc, M., and Büchler, M. W. (1997) Enhanced expression of urokinase plasminogen activator and its receptor in pancreatic carcinoma. *Br. J. Cancer 75*, 388−395.
(15) Ma, Y. Y., and Tao, H. Q. (2012) Role of urokinase plasminogen activator receptor in gastric cancer: a potential therapeutic target. *Cancer Biother. Radiopharm. 27*, 285−290.
(16) Li, D., Liu, S., Shan, H., Conti, P., and Li, Z. (2013) Urokinase plasminogen activator receptor (upar) targeted nuclear imaging and radionuclide therapy. *Theranostics 3*, 507−515.
(17) Mazzucchelli, S., Colombo, M., Verderio, P., Rozek, E., Andreata, F., Galbiati, E., Tortora, P., Corsi, F., and Prosperi, D. (2013) Orientation-controlled conjugation of HALO-fused homing peptides to multifunctional nanoparticles for specific recognition of cancer cells. *Angew. Chem., Int. Ed. 52*, 3121−3125.
(18) Bhattacharyya, S., Singh, R. D., Pagano, R., Robertson, J. D., Bhattacharya, R., and Mukherjee, P. (2012) Switching the targeting pathways of a therapeutic antibody by nanodesign. *Angew. Chem., Int. Ed. 51*, 1563−1567.
(19) Huang, Y.-F., Liu, H., Xiong, X., Chen, Y., and Tan, W. (2009) Nanoparticle-mediated IgE-receptor aggregation and signaling in RBL mast cells. *J. Am. Chem. Soc. 131*, 17328−17334.
(20) Häkkinen, H. (2012) The gold−sulfur interface at the nanoscale. *Nat. Chem. 4*, 443−455.
(21) Hosta-Rigau, L., Olmedo, I., Arbiol, J., Cruz, L. J., Kogan, M. J., and Albericio, F. (2010) Multifunctionalized gold nanoparticles with peptides targeted to gastrin-releasing peptide receptor of a tumor cell line. *Bioconjugate Chem. 21*, 1070−1078.
(22) (a) Yang, S.-J., Lin, F.-H., Tsai, K.-C., Wei, M.-F., Tsai, H.-M., Wong, J.-M., and Shieh, M.-J. (2010) Folic acid-conjugated chitosan nanoparticles enhanced protoporphyrin IX accumulation in colorectal cancer cells. *Bioconjugate Chem. 21*, 679−689. (b) Ventola, C. L. (2012) The nanomedicine revolution. Part 2: Current and future clinical applications. *P T 37* (10), 582−591. (c) Thakor, A. S., Luong, R., Paulmurugan, R., Lin, F. I., Kempen, P., Zavaleta, C., Chu, P., Massoud, T. F., Sinclair, R., and Gambhir, S. S. (2011) The fate and toxicity of Raman-active silica−gold nanoparticles in mice. *Sci. Transl. Med. 3* (79), 79ra33. (d) Paciotti, G. F., Myer, L., Weinreich, D., Goia, D., Pavel, N., McLaughlin, R. E., and Tamarkin, L. (2004) Colloidal gold: a novel nanoparticle vector for tumor directed drug delivery. *Drug Delivery 11*, 169−183.
(23) Karakoti, A. S., Das, S., Thevuthasan, S., and Seal, S. (2011) PEGylated inorganic nanoparticles. *Angew. Chem., Int. Ed. 50*, 1980−1994.
(24) Gao, J., Huang, X., Liu, H., Zan, F., and Ren, J. (2012) Colloidal stability of gold nanoparticles modified with thiol compounds: bioconjugation and application in cancer cell imaging. *Langmuir 28*, 4464−4471.
(25) Swartz, J. D., Gulka, C. P., Haselton, F. R., and Wright, D. W. (2011) Development of a histidine-targeted spectrophotometric sensor using Ni(II)NTA-functionalized Au and Ag nanoparticles. *Langmuir 27*, 15330−15339.
(26) Krpetic, Z., Davidson, A. M., Volk, M., Levy, R., Brust, M., and Cooper, D. L. (2013) High-resolution sizing of monolayer-protected gold clusters by differential centrifugal sedimentation. *ACS Nano 7*, 8881−8890.
(27) Turkevich, J., Cooper Stevenson, P., and Hillier, J. (1951) A study of the nucleation and growth processes in the synthesis of colloidal gold. *Discuss. Faraday Soc. 11*, 55−75.
(28) Turkevich, J., Stevenson, P. C., and Hillier, J. (1953) The formation of colloidal gold. *J. Phys. Chem. 57*, 670−673.
(29) Frens, G. (1973) Controlled nucleation for the regulation of the particle size in monodisperse gold suspensions. *Nat. Phys. Sci. 241*, 20−22.
(30) Pensa, E., Cortes, E., Cortney, G., Carro, P., Vericat, C., Fonticelli, M. H., Benitez, G., Rubert, A. A., and Salvarezza, R. C. (2012) The chemistry of the sulfur−gold interface: in search of a unified model. *Acc. Chem. Res. 45*, 1183−1192.
(31) Colombo, M., Mazzucchelli, S., Collico, V., Avvakumova, S., Pandolfi, L., Corsi, F., Porta, F., and Prosperi, D. (2012) Protein-assisted one-pot synthesis and biofunctionalization of spherical gold nanoparticles for selective targeting of cancer cells. *Angew. Chem., Int. Ed. 37*, 9272−9275.
(32) Scari, G., Porta, F., Fascio, U., Avvakumova, S., Dal Santo, V., de Simone, M., Saviano, M., Leone, M., del Gatto, A., Pedone, C., and Zaccaro, L. (2012) Gold nanoparticles capped by a GC-containing peptide functionalized with an RGD motif for integrin targeting. *Bioconjugate Chem. 23*, 340−349.
(33) Ma, L. L., Tam, J. O., Willsey, B. W., Rigdon, D., Ramesh, R., Sokolov, K., and Johnston, K. P. (2011) Selective targeting of antibody conjugated multifunctional nanoclusters (nanoroses) to epidermal growth factor receptors in cancer cells. *Langmuir 27*, 7681−7690.
(34) Jiang, W., Kim, B. Y. S., Rutka, J. T., and Chan, W. C. W. (2008) Nanoparticle-mediated cellular response is size-dependent. *Nat. Nanotechnol. 3*, 145−150.
(35) Tu, Y., Wu, P., Zhang, H., and Cai, C. (2012) Fluorescence quenching of gold nanoparticles integrating with a conformation-switched hairpin oligonucleotide probe for microRNA detection. *Chem. Commun. 48*, 10718−10720.
(36) Dulkeith, E., Ringler, M., Klar, T. A., Feldmann, J., Munoz Javier, A., and Parak, W. J. (2005) Gold nanoparticles quench fluorescence by phase induced radiative rate suppression. *Nano Lett. 5*, 585−588.